Journal of Particle Science and Technology 3 (2017) 197-209

J | P | S | T

http://jpst.irost.ir

Journal of Particle Science and Technology

IROST

Maltodextrine nanoparticles loaded with polyphenolic extract from apple industrial waste:Preparation, optimization and characterization

Shohreh Saffarzadeh-Matin*, Majid Shahbazi

Department of Chemical Technologies, Iranian Research Organization for Science and Technology (IROST), Tehran, Iran

HIGHLIGHTS

- Maltodextrine with low hydrolytic conversion (DE: 8) was utilized as the wall material.
- RSM was utilized for the modeling and optimization of three independent variables.
- The surfactant concentration and the mixture intermixing were significant factors.
- Spherical shaped NPs with a size of 52 nm with a loading efficiency of 98% were produced.
- Hydrogen bonding is the main mode of interaction between the core and the shell.

GRAPHICAL ABSTRACT

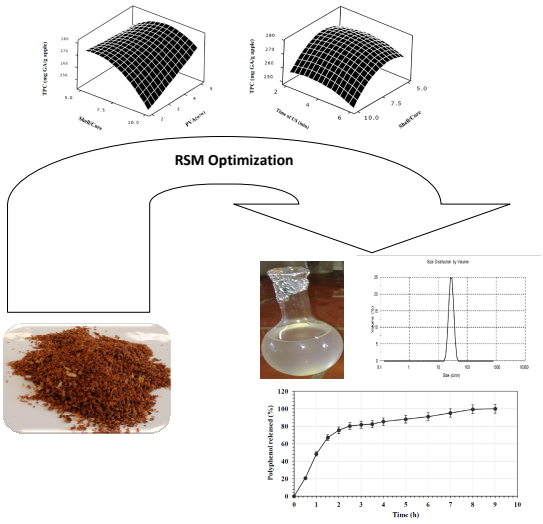

ARTICLE INFO

Article history:

Received 25 November 2017
Revised 19 December 2017
Accepted 27 January 2018

Keywords:

Process optimization
Natural polymers
Nanoencapsulation
Apple pomace polyphenolic extract
Nanoprecipitation

ABSTRACT

The main aim of this study was to prepare apple pomace polyphenolic extract (APPE-referred to as a core) loaded into biodegradable and commercially available natural polymer such as maltodextrin (MD-referred to as a shell). The polymer coating potentially improves its low stability and bioavailability and also directs the control release of the encapsulated material. The MD-nanoparticles (NPs) loaded with the APPE were prepared by a modified nanoprecipitation method. An experimental central composite design was utilized for the modeling, optimization and to assess the influence (and interactions) of the shell to core ratio, surfactant concentration, and sonication time (as the independent variables) on the NPs preparation to maximize the level of polyphenols loading and the NPs formation yield (referred to as dependant variables). The adopted models were verified statistically and experimentally. The results showed that amongst the independent variables, the shell to core ratio and the surfactant concentration were statistically significant in the experimentally selected ranges. By adopting the optimal process conditions, the spherical shaped NPs were prepared with a mean average size of 52 nm (confirmed by the Dynamic Light Scattering and FE-SEM techniques) and polyphenols loading efficiency of 98%. FT-IR spectroscopy confirmed the successful entrapment of the core in the shell of NPs. Hydrogen bonding is one of the modes of interactions between the hydrophilic moieties of polyphenols and MD. The in vitro polyphenols release of the NPs through simulating cancerous tumor acidity conditions represented a sustainable release, indicating potential anticancer application of the NPs.

* *Corresponding author: Tel.: +9821-56276637 ; Fax: +9821-56276265 ; E-mail address: saffarzadeh@irost.ir*

DOI: 10.22104/JPST.2018.2612.1100

1. Introduction

Polyphenols with natural origins e.g., apple pomace polyphenols could be potentially used as food supplements, pharma- and cosmeceuticals due to their antimicrobial, antiradical and antioxidant activities [1,2]. The significance of these natural antioxidants in preventative medicine, particularly for reducing cancer risk, is well known and has been the subject of recent reviews [3]. The high activity of natural polyphenols makes them prone to chemical instability against environmental conditions such as oxygen, moisture, etc. Moreover, most natural polyphenols show low in vivo bioavailability and solubility, which may weaken or even suppress their full beneficial health effects [4]. In this regard, nanoencapsulation of polyphenols, i.e., their incorporation into biodegradable natural polymers, not only enhances their chemical stability but also provides passive and active targeting and controlled release [5]. Additionally, their low in vivo bioavailability and solubility will be improved considerably [6], which affects their absorption by the gastrointestinal system [7]. For example, the recent substantial research conducted on the nanoencapsulation of curcumin [8-10] and quercetin [11-13] as model polyphenols are indicative of the importance of this new emerging technology in preventative medicine. By adopting a biomimicry approach it is believed that polyphenolic compounds, e.g., green tea polyphenols, act synergistically together as their nature's pattern. Therefore their mixed extraction, purification, and bioavailability have been the subject of intensive research over recent years [14,15].

The main objective of this study was to identify the most suitable operating conditions for the green production of natural polymer based-nanoparticles loaded with polyphenol extract produced from Iranian industrial apple pomace.

Apple is one of the most frequently consumed fruit in the Iranian diet. According to the latest FAOSTAT report (2012), the total worldwide production of apple is approximately 60-70 million metric tons (MMT)/ annually, and the Iranian contribution is about 5% (above 3 MMT) of this production, making it the fourth largest world producer. In Iran apples are mostly consumed fresh and roughly 0.57 MMT are processed into juice, jams, and syrup [16]. Therefore, during the processing of apple products a considerable amount of industrial apple waste is produced annually in Iran. This waste is mostly used as animal feed. The recovery of value added natural by-products from industrial wastes e. g., apple pomace, is a global research trend to reduce environment pollution in addition to increase profitability [3,17]. According to a study conducted on the polyphenol profile of the mixture of flesh and peel of the main Iranian apple cultivars [18], the main constituents were (-)-epicatechin, cyanidin-3-galactoside, quercetin-3-galactoside followed by chlorogenic acid and phloridzin dehydrate (Figure 1).

In the encapsulation process varieties of natural and/or synthetic polymers could be used as a matrix and/or coating to retard the diffusion of oxygen and/ or small organic molecules, which further leads to oxidative stability [19]. Polysaccharides such as maltodextrin, chitosan and cellulose are examples of such wall compounds [20], e.g., chitosan was used as wall material for encapsulation of a natural antioxidant extracted from yerba mate [21].

However, use of the MD (high DE: 18-20) is restricted as an appropriate shell material due to its low glass transition temperature (Tg). Low Tg may prompt crystals formation under increasing temperature, for example during the storage period and also the applications [22]. Therefore, the structural integrity of the particles will be disrupted and premature release of the encapsulated active components will occur [23]. In this study, MD with low hydrolytic conversion (DE: 8) was utilized as the wall material. We propose that a lower DE value increases the MD polymer solubility in organic polar solvents and reduces its water solubility. These will presumably result in a more rapid precipitation, greater encapsulation efficiency, and finally potential higher stabilization during the storage period.

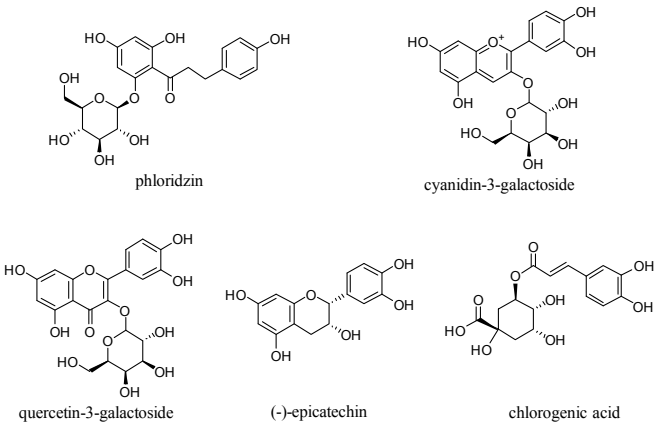

Fig. 1. Chemical structure of main polyphenolic constituents of industrial apple pomace.

In this study the nanoprecipitation method was utilized for the fabrication of the novel MD- APPE composite NPs. Nanoprecipitation is a straightforward process which generates a narrow unimodal size distribution of NPs [24] and is mostly suitable for hydrophobic compounds [25]. However, the amphiphilic character of various mixed polyphenolic compounds (due to the presence of both aromatic rings and hydroxyl groups) make the suitability of the nanoprecipitation method questionable as the technique of choice for the encapsulation. Therefore, high molecular weight polyvinyl alcohol (dissolved into water) was used as surfactant to reduce (or even zeroing) the polyphenolics leakage towards the aqueous phase.

Low power sonication homogenization was used to improve the solvent-nonsolvent intermixing due to its increasing the aqueous phase viscosity. The operating conditions were expressed in terms of the wall to the core ratio, the surfactant concentration (w/w %) and the sonication homogenization time (as independent variables) to maximize the entrapment of the apple pomace polyphenol extract and the NPs formation yield (as response variables).

In this study a 33-full factorial design and RSM were employed to investigate the interactions as well as the optimization of the variables. RSM has been recently adopted and used in the optimization of encapsulation process of various natural polyphenols [26,27].

2. Experimental

2.1. Materials

Maltodextrin (DE: 8, Mw: 15,000 g mol-1) was supplied by Arian glucose CO (Iran). Ethanol (96%) was obtained from the Zakaria Jahrom Institute (Iran). Folin Ciocalteu's phenol reagent, Gallic acid, and polyvinyl alcohol (Mw: 72000 g mol-1) were obtained from Merck Chemical Co (Germany). All other reagents were of analytical grade. Deionized water was used in all experiments.

Apple pomace including the peel and seeds was provided immediately after processing in October, 2015 by the Sanich Co. (Iran). The waste was transferred within a few hours to a laboratory, dried in an air flow cabinet oven at 30 °C for 48 h, and powdered in a hammer mill crusher. The ground material was consecutively passed through the sieves of various mesh sizes and the fraction between 35 and 60 mesh sizes (a mean particle size of 0.25-0.50 mm) was collected for further processing. The sized material was placed in an opaque plastic bag and stored at room temperature (20-25 °C) in a dry ventilated area until used.

2.2. Methods

2.2.1. Determination of total phenolic compounds (TPC)

The method used to determine the TPC employed Folin-Ciocalteu (FC) reagent; this was done according to a procedure described in the literature [28]. Six different concentrations of Gallic acid solutions (25–500 mg/l) were used for the calibration plot. The estimation of phenolic compounds was carried out in triplicate, and the results were averaged (standard deviations <5%). The results were expressed in Gallic Acid (GA) equivalents (mg GAE/g waste). The measurements were carried out by ultraviolet absorption at their maximum wavelength on a MESU LAB UV/V-3000 spectrophotometer, Hong Kong.

2.2.2. Extraction of phenolic compounds

40 g of the powdered apple waste was placed into individual cotton bags in the five cells of a multistage counter current extraction system. For extraction ethanol concentration of 45%, solvent to dry waste ratio of 10, extraction temperature of 65 °C and extracting time of 6 h were selected. Multi stage counter current extraction was performed according to a procedure previously reported [29]; then the extracts produced from each stage were mixed and filtered. The filtrate was further concentrated via evaporation under reduced pressure and further subjected to spray drying [30]. 10 mg of the dry extract was dissolved in 25 ml of hydroethanol of 50% and was analyzed for TPC, which was 288 mg/l GA.

2.2.3. Preparation of the NPs containing apple pomace polyphenols

Accurately weighed amounts of the MD (selected from experimental arrangements designed using RSM (Table 1) and dried APPE (20 mg) were magnetically stirred (Model EM3300T, Labotech Inc., Germany) overnight in ethanol 96% (8 ml) at room temperature.

The colloidal solution was then added to 15 ml of water containing accurately weighed amounts of polyvinyl alcohol as surfactant (selected from Table 1, magnetically stirred and dissolved at 70 °C temperature). Upon dilution with water, a dispersion of NPs was generated instantaneously. The latter was immediately sonicated with 150 W power by using a prob sonicator for the defined times, according to the experimental arrangements designed using RSM (Table 1).

The produced NPs were further collected by ultracentrifugation 3 times (Model 29318, Sigma, Laborzentrifugen GmbH, Germany) at 13500 rpm for 45 min, the supernatants were mixed and analyzed for the TPC. Therefore, the difference between the total amount used to prepare the nanopaticles and the amount that was found in the supernatant was attributed to the amount of polyphenols loaded within the NPs. The collected particles were washed twice with 5 ml of hydro-ethanol 50% (v/v) and subjected to drying using a vacuum oven (Model 3737, Precision Scientific, INC,) at 40 °C and weighed. The filtrates were analyzed for TPC. There was no detectable polyphenols in the washing filtrates as evidenced by TPC analysis, suggesting that polyphenols did not exist on the NPs surfaces. The vacuum dried particles were stored at 4 °C until used for other characterizations.

2.3. Ultrasonic generator

The equipment employed in this search was a 20 kHz, 600 W ultrasonic generator, MISONIX Ultrasonic liquid Processor, Model S-4000 (Qsonica, LLC, USA) and a titanium microtip 419 BR as the probe.

2.4. Loading efficiency, polyphenol loading content and NPs' yield

The percentages of loading efficiency (% L.E), polyphenol loading content (% LC) and the NPs yield (% N.Y) were calculated according to equations Eqs. (1), (2) and (3), respectively. The N.Ys' were obtained gravimetrically.

$$\text{L.E} = (\text{TPC of the NPs}/\text{TPC of the feeding sample}) \times 100 \quad (1)$$

$$\text{L.C} = (\text{weight of polyphenol in the NPs}/\text{the weight of NPs}) \times 100 \quad (2)$$

$$\text{N.Y} = (\text{the weight of NPs} / \text{the weight of feeding polymer and sample}) \times 100 \quad (3)$$

The polyphenols loaded in nanospheres expressed as mg GAE/L were also quantified by the Folin-Ciocalteu method after dissolving 50 mg of NPs in 20 ml acetone.

Table 2. Independent variables and coded values employed for optimization of the nanoparticle preparation procedure.

Independent variables	Factor units	level		
		-1	0	1
Shell to core	X_1	5	7.5	10
Surfactant (w/w %)	X_2	2	3.5	5
Time of ultrasonic homogenizaton (min)	X_3	2	4	6

2.5. Experimental design

The Minitab Version 16 software was used to conduct the experimental design and the statistical analysis. A three factor and three levels second order regression for the central composite design (CCD) in RSM that consisted of 20 experimental runs was employed. This was not only used to evaluate the interaction of targeted variables, but also to optimize the TPC and the NPs yield (% N.Y) as response variables. The coded values, levels, and real values are listed in Table 1. Regression analysis was performed to establish an empirical second-order polynomial model through Eq. (4).

$$Y = \beta_0 + \sum_{i=1}^{3} \beta_i X_i + \sum_{i=1}^{3} \beta_{ii} X_i^2 + \sum_{i=1}^{3} \sum_{j=i+1}^{3} \beta_{ij} X_i X_j \quad (4)$$

where Y is the predicted response variable, β_0 is defined as the constant, β_i is the linear coefficient, β_{ii} is the square coefficient, and β_{ij} is the cross-product coefficient. X_i and X_j are two independent variables.

2.6. Characterization of the MD- APPE NPs: Size distribution and morphology of the nancapsules

The particle size distribution of NPs was determined by dynamic light scattering (DLS) measurement using Zetasizer nano ZS instrument (Malvern Instruments Ltd, United Kingdom). The appropriate concentration

of the sample was prepared with the deionized water, and then was filtered with a 0.45 mm Millipore filter, before analysis.

The shape and the surface morphology of NPs were observed by TESCAN WEGA3-SB scanning electron microscopy (FE-SEM).

2.7. FTIR spectrum analysis

Each powdered sample was mixed with KBr salt, using a mortar and pestle, and compressed into a thin pellet. Fourier transform infrared (FTIR) spectroscopy experiments were performed on a Perkin-Elmer (model: Spectrum-1) over a frequency window from 4000-400 cm^{-1}. Interferograms (64) with a resolution of 4 cm^{-1} were co-added and Fourier transformed for each sample and background.

2.8. In vitro polyphenols release of polyphenol loaded NPs

In vitro release studies of polyphenols from the NPs were performed by diffusion technique. Nanospheres (50 mg) inside a cellulose dialysis bag (10 cm, dialysis tubing, molecular weight (Mw) cut off 12,000 Da, Sigma-Aldrich) were suspended inside a beaker containing 100 ml of a release medium consisting of buffer (pH 4.5 and 6.8) at 37 °C and 125 rpm (Brunswick INNOVA 4430 incubator shaker, GMI.inc, USA). The NPs suspensions were aliquoted in 1.5 ml centrifuge tubes in time intervals of half an hour for the first 4 h, an hour for the next 6 h and finally two hours for the third 8 h, centrifuged at 15,000 rpm for 10 min, then decanted and the supernatant was utilized to quantify the in vitro release profile of polyphenols in slight acidic environment models , i.e. pH 4.5 (Acetate Buffer Saline) and pH 6.8 (Phosphate Buffer Saline) using the Folin-Ciocalteu method as described previously. All experiments were carried out in triplicate.

3. Results and discussion

3.1. Fitting the response surface models and models verification for the responses

Independent variables and coded values employed for optimization of the nanoparticle preparation procedure are presented in Table 1. The design arrangement and experimental results of the nanoparticle formation are shown in Table 2. The multiple regression coefficients were calculated using Minitab 16 software for both responses. By applying the coefficients into the generalized model (Eq. (4)), the second order polynomial equations for the acquired TPC (Eq. (5)) and the NPs yield (Eq. (6)) were obtained in terms of coded values of shell to core ratio (X_1), surfactant weight percentage (X_2), and time of the sonication homogenization (X_3).

$$Y_1 = 179.83 + 19.67X_1 + 2.58X_2 + 14.02X_3 - 1.93X_{12} - 0.98X_{22} - 1.53X_{32} \quad (5)$$

$$Y_2 = 49.40 + 4.79X_1 - 0.83X_2 + 4.28X_3 - 0.48X_{12} - 0.06X_{22} - 0.36X_{32} - 0.52X_1X_2 - 0.04X_1X_3 - 0.41X_2X_3 \quad (6)$$

Table 2. The arrangement and responses of the three-factor, three-level second-order regression for central composite design.

Run order	Shell to core (X_1)	Surfactant (% w/w)	Time of sonication (min)	TPC (mg GAE/l)	N.E. (%)
1	7.5 (0)	3.5 (0)	4 (0)	280.56	73.62
2	7.5 (0)	3.5 (0)	6 (1)	270.47	70.98
3	10 (1)	3.5 (0)	4 (0)	265.22	69.60
4	5 (-1)	2 (-1)	6 (1)	267.67	70.76
5	7.5 (0)	3.5 (0)	4 (0)	272.44	71.50
6	7.5 (0)	3.5 (0)	2 (-1)	275.11	72.19
7	10 (1)	5 (1)	6 (1)	256.89	67.41
8	10 (1)	2 (-1)	6 (1)	238.67	62.63
9	10 (1)	2 (-1)	2 (-1)	234.67	61.58
10	7.5 (0)	3.5 (0)	4 (0)	280.113	71.64
11	7.5 (0)	3.5 (0)	4 (0)	278.11	72.98
12	7.5 (0)	2 (-1)	4 (0)	276.56	73.10
13	5 (-1)	3.5 (0)	4 (0)	268.56	70.47
14	10 (1)	5 (1)	2 (-1)	265.78	72.37
15	7.5 (0)	3.5 (0)	4 (0)	279.56	66.54
16	5 (-1)	2 (-1)	2 (-1)	266.33	69.89
17	5 (-1)	5 (1)	6 (1)	261.89	68.72
18	5 (-1)	5 (1)	2 (-1)	273.56	71.78
19	7.5 (0)	5 (1)	4 (0)	276.89	72.66
20	7.5 (0)	3.5 (0)	4 (0)	279.67	73.39

The estimation of phenolic compounds was carried out in triplicate, and the results were averaged (standard deviations <5%).

The analysis of variance (ANOVA) result (summary tables for TPC and N.Y %) used to check the adequacy of the developed models is presented in Table 2. From the ANOVA table, it can be seen that the models were significant and adequate at a 95% confidence level. The similarity between the experimental values and the predicted ones (using the models) for both response variables were another indication of satisfactory models. According to the summary table of ANOVA (Table 3), the calculated F-value of the lack of fit for both TPC (3.31) and N.Y % (3.33) did not exceed the tabulated values of the F-distribution (3.5) found from the standard table at the 95% confidence level. This implies that for both models, the lack of fit is not significant ($p>0.05$) relative to the pure errors; therefore, both models were statistically significant and the responses were optimized.

On the other hand, the F-values from the regression models (16.11 for TPC and 12.22 for N.Y %), which are the calculated values using the adjusted mean square of regression models divided by the adjusted mean square of the residual errors, are more than 1. This indicated that there were significant differences between the models data and the mean values, which were not due to sampling or experimental error (rejecting the null hypothesis). So the experimental values of TPC (Y_1) and N.Y % (Y_2), as dependent variables, were fitted to the second-order polynomial equations using RSM as shown in Eqs. (3) and (4). It is worth mentioning that the coefficients of the determinations (R^2) of TPC and N.Y % were 0.935 and 0.917, respectively, which were another indication that both models adequately fit the chosen parameters.

The absolute values indicated that the shell to core (X_1) followed by time of the sonication homogenization (X_3) and the weight percentage of surfactant (X_2) are the significant factors affecting both the acquired TPC loaded within the MD and nanoparticle formation yield.

3.2. Analysis of response surfaces for the responses

The three-dimensional response surfaces of four independent variables were obtained by keeping two of the variables constant. The constants were equal to the natural value of the zero level. The response surfaces for TPC and N.Y % are shown in Figures 2(a-c) and (a'-c'), respectively.

The most important results are outlined as:

1-The combined effect of the surfactant concentration and the shell/core ratio variables on the acquired TPC loaded within the NPs, (Figure 2a), indicates in the range of the surfactant concentration as low as 2-3.5% w/w and the core/shell ratio from 5-8 that the polyphenol loading value remains relatively constant and high (275-280 mg GAE/l), and then starts to decrease as the core/shell ratio increases up to 10. The highest level of loaded polyphenols (maximum TPC value) was obtained in the shell/core ratio ranging of 6-7.5 and the surfactant concentration more than 4% w/w.

Under controlled conditions, after the addition of the organic solvent to the nonsolvent, a dispersion of NPs is generated instantaneously by spontaneous diffusion of the solvent in the aqueous phase. Moreover, as the polymer concentration in the organic phase increases, a high viscosity of the polymeric solution prevents the appropriate organic phase diffusion towards the aqueous phase, so the coprecipitation of the maltodextrin/polyphenol solution into water was restricted and the level of TPC loading was decreased. This was consistent with the results gained by other studies [31]. This result also shows that in this critical point, due to the presence of the surfactant in the aqueous phase, the interfacial

Table 3. Summary table of analysis of variance for TPC and NY %.

	TPC					N.Y %			
Source	DF	Adj. SS	Adj. MS	F	P	Adj. SS	Adj. MS	F	P
Regression	9	2881.55	320.173	16.11	0.00	188.63	20.96	12.22	0.00
Residual Error	10	198.72	19.87			17.15	1.71		
Total	19	3080.27				205.79			
Lack of fit	5	152.65	30.53	3.31	0.11	13.187	2.64	3.33	0.11
R-Sq		93.55				91.67			
R-Sq (adj)		87.74				84.17			

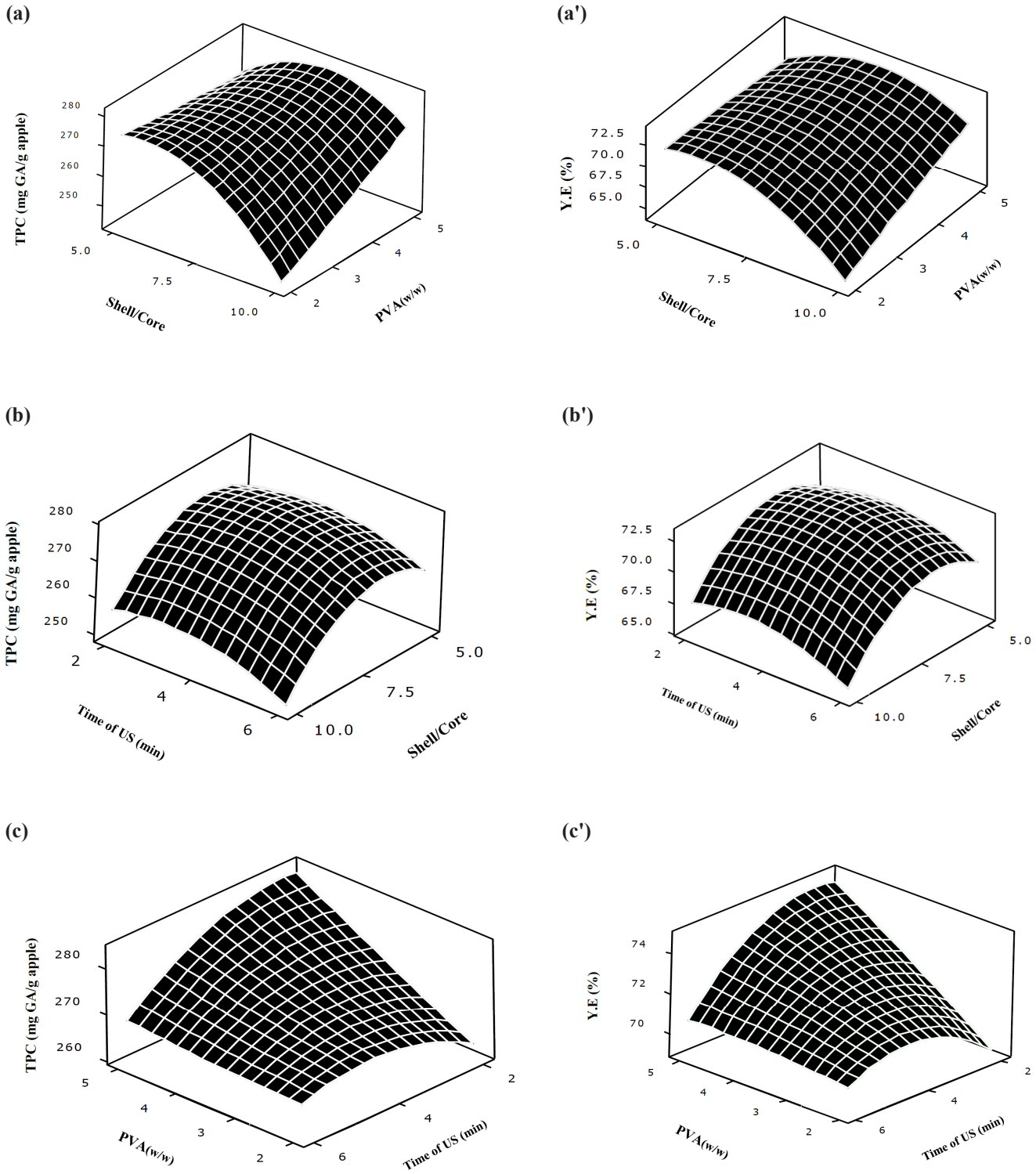

Fig. 2. Response surface plots of the combined effect of shell-to-core ratio and surfactant (PVA) concentration (a), shell-to-core ratio and time of sonication (b), PVA concentration and time of sonication (c) on the TPC of loaded NPs, shell-to-core ratio and PVA concentration (a'), shell-to-core ratio and time of ultrasonication (b'), PVA concentration and time of sonication (c') on the yield of NPs preparation.

tension between two liquids is appropriately lowered and the organic phase diffusion towards the aqueous phase is improved, leading to the highest level of TPC loading. However, the high viscosity of the aqueous phase would also hamper the diffusion of the organic solvent; therefore, the surfactant/ polymer ratio must be carefully optimized [32]. This mechanism is more prominent at medium and high polyvinyl alcohol concentrations (more than 7%). The critical influence of the type and the concentration of various surfactants, e.g. polyvinyl alcohol, on nanoparticles loaded with silymarin as a hydrophobic compound using the

nanoprecipitation method has been investigated [33].

2- Figure 2b shows the combined effect of the sonication time and the shell/core ratio variables on the acquired TPC. It indicates as the shell/core increases, during nearly the entire range of the time of sonication, the polyphenol loading decreases. This clearly indicates the negative effect of increasing the polymer concentration, attributed to a shell/core ratio more than 7, in preventing the appropriate organic phase diffusion into the aqueous phase despite the sonication/ enforced (helped) stirring. However, a maximum peak is observed in the shell/core 6.6-6.8 and the sonication time of 3.7-3.9 min, which is attributed to a polyphenol loading level more than 95%.

This result indicates the positive effects of moderate homogenization time in polyphenols loadings via the nanopercipitation method. The positive influence of the solvent-nonsolvent intermixing to reduce the mean NPs diameter during the nanopercipitation process has already been investigated [34,35].

The interaction effect of the surfactant concentration and the sonication time variables on the acquired TPC, (Figure 2c), indicates as the surfactant concentration increase in the range of the sonication time between 2-5 min, the polyphenol loading increases, until a maximum peak is observed in the moderate surfactant concentration of 4-5% w/w and the sonication time of 2-4.2 min.

This observation might be attributed to a less favorable mixing efficiency during the sonication/homogenization process resulting from a higher viscosity of the aqueous phase, above a critical concentration of surfactant. The less favorable mixing efficiency in a higher viscosity of the aqueous phase has been already reported [32]; however, it has neither been optimized nor its interaction with other variables been studied.

Interestingly the relatively same patterns (in terms of rises and falls) were observed with the nanoparticle formation yield (Figures 2(a'-c')), meaning that both dependant (response) variables were directly correlated and followed the same trends upon the programmed variations in the independent variables. This correlation has not been previously reported.

Our study showed that in a critical surfactant concentration an interfacial tension lowering effect is observed. This finding also showed the constructive influence of the solution-nonsolvent intermixing in the particle size distribution of NPs, the level of loading efficiency, and the formation yield of the NPs. On the other hand, the sonication homogenization transforms the maltodextrin solution into small droplets immediately after entering the water, leading to acceleration of the solvent-nonsolvent intermixing process. Moreover the possible formation of large aggregates due to flocculation of particles is overcome, which leads to NPs with unimodal size distributions and low polydispersity. Furthermore, the sonication homogenization as well as the surfactant application lowered the NPs growth in the initial steps; leading to finer NPs. Our observation is in contrast with research that reported no substantial improvement in the diffusion rate of organic solvent towards aqueous solvent in the surfactant presence. These results are not clearly in agreements with some of the principles of the common nanoprecipitation models based on the so-called "Marangoni effect" in which interfacial tension and mechanical turbulence were not considered as the driving forces during the course of the NPs formation [36].

3.3. Optimization of the NPs formation process

To achieve the maximum level of TPC and NPs formation yield, the optimal level of extraction parameters were generated based on both two separate single response variables and in combination. Multiple graphical and numerical optimizations were run to determine the optimum level of the independent variables, with desirable response targets, and further verified experimentally. The optimal conditions were expressed as the wall to core ratio of 7.5, the percentage of surfactant of 4% w/w, and the time of sonication homogenization of 2 min. The NPs were prepared in triplicate according to the optimal conditions to assess the experimental reproducibility and the models verification. The response surface models were verified by similarities between the observed and the predicted values. For the NPs obtained experimentally in optimal process conditions, the L.E of 98% , the L.C of 8.62 % and the N.Y of 75% were quantified according to the Eqs. (1-3), respectively.

The DLS result on these NPs showed a mean particle size of 52 nm with the 40 nm distribution width (Figure 3a), which was composed of just one population, corresponding to 100% of all particles. This is less than the previously reported studies on PLA-grape extract NPs, which was 351.9 and 291.6 nm for the seed and

skin grape extracts, respectively [37]; and also (PLGA-PEG) NPs loaded with pomegranate extract, which was in the range of 120-200 nm [38]. Both NPs were prepared by the modified emulsion-solvent evaporation method. It seems that presumably at the initial stage of the nanoprecipitation process, sonication inhibited the crystal growth. Then it was followed by adsorption of the polyvinyl alcohol on to the NPs, leading to further inhibition growth and producing finer NPs. This would certainly influence their final bioavailability due to the higher surface to volume ratio.

The FE-SEM micrographs of NPs' suspension (Figure 3b) showed a spherical shape of the dispersed particles with smooth surfaces, and the NPs sizes were in agreement with the results governed by DLS measurements.

3.4. Fourier Transform Infra-Red (FT-IR) characterization of MD-APPE NPs

The MD, the APPE, and the loaded NPs were evaluated by FT-IR spectroscopy to identify the functional groups of the active components and also any mode of interactions between the polymeric wall and the polyphenolic core. The resulting spectrums are shown in Figure 4. For the APPE, the major peaks were assigned to the stretching vibration of hydroxyl groups (a broad band around 3390 cm^{-1}), asymmetrical stretching vibration of CH_2 groups ($\nu(CH_2)$ 2928 cm^{-1}) , accompanied by the corresponding $\delta(CH_2)$ bending vibration (1350, 1226, and 632 cm^{-1}), −CO stretching (1727 cm^{-1}), and aromatic bending and stretching (ν(C−C) conjugated with C=C (1350 cm^{-1}) and ν(C=C) (1615 cm^{-1}). Additionally, two peaks at lower wave numbers were assigned to C−H and C−C out of plane bending vibrations at 875 and 776 cm^{-1}, respectively, which are associated with 1, 4-disubstituted benzene molecules [39]. A very strong broad peak at 1051 cm^{-1} corresponds to the ν(C−O−C), which is associated with the glycosydic bond.

As it is clearly shown in Figure 4 and Table 4, the wave numbers of the major peaks of the APPE (c) and MD (b) were shifted in the NPs (a) and also their intensities were changed. A very strong broad peak correspondent to the glycosydic bond at 1051 cm^{-1}

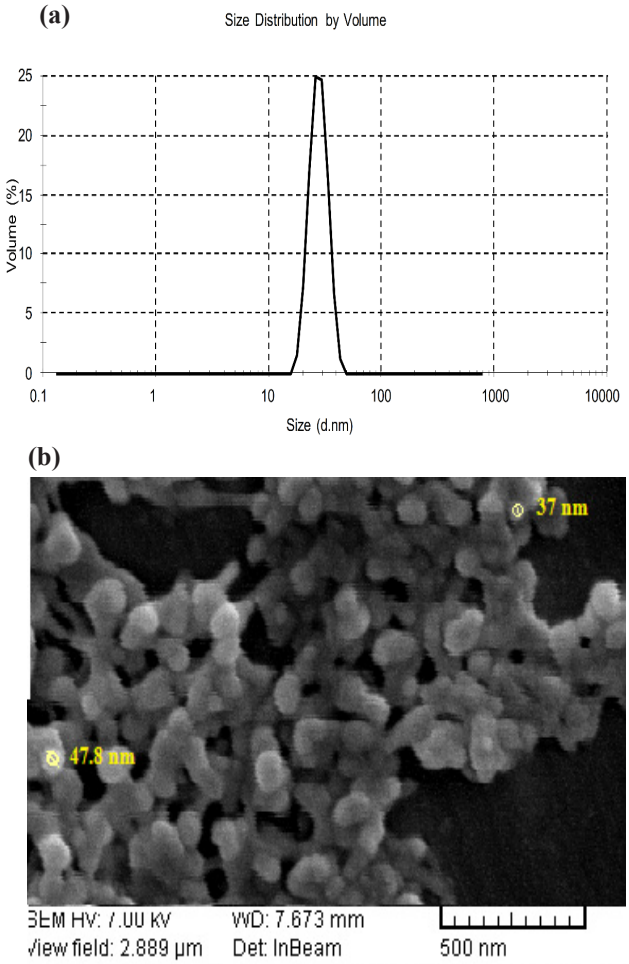

Fig. 3. Particle size spectrum of MD-APPE NPs, DLS result (a), FE-SEM image (b).

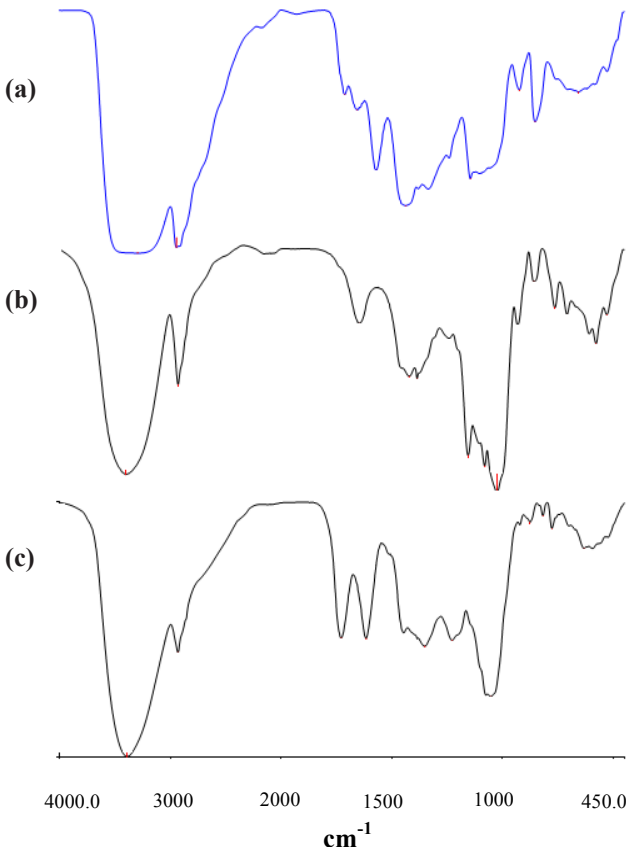

Fig. 4. FT-IR spectra of MD-APPE NPs (a), MD (b) and APPE (c).

was absent in the NPs. These observations indicate the successful entrapment and also an interaction between the wall and the core. Hydrogen bonding is suggested as one of the mode of interactions between the hydrophilic moieties of polyphenols and MD. The hydrogen bonds can be formed between the hydroxyl groups of APPE and MD (intra- and inter-chain bonds) or between the hydroxyl groups of polymer chains and surfactant molecules [13].

3.5. In-vitro release of MD-APPE NPs, simulating cancerous tumor acidity conditions

Figure 5 presents the release profile of MD-APPE NPs under mild acidic conditions (pH 4.5, 6.8). Both simulations represented a sustainable release of MD-APPE NPs and also the higher release rate of phenolics in pH 4.5 than pH 6.8, prolonged to 9 and 15 h, respectively. This shows an initial burst release on average of 50-65% and 70-80% of APPE within 2-3 h at pH 6.8 and 4.5, respectively. An initial burst release of the nanoencapsulated polyphenols were also reported by other studies, which was attributed to the fraction of active component placed near the surface of the NPs [37,40] .

The MD-APPE nanoparticles with the sustainable release ability produced in this study could be considered as a potential candidate to target certain cancerous tumors, e.g. colon cancer. Application of the pH-sensitive polymeric NPs loaded with an anticancer drug to target solid tumors with slightly acidic extracellular pH (pH 4.5-6.8) environment has been reviewed [41]. However, more specific in vitro and in vivo experiments are necessary to shed more light into the feasibility of this potential application.

Table 3. FT-IR major peaks assignments of the APPE, the MD and the loaded NPs.

Assignment	APPE	MD	NPs
ν(O−H···O)	3390 (s,b)	3398 (s,b)	3291 (s,b)
ν_a(CH_2)	2928 (s)	2925 (s)	2940 (s)
ν_s(CH_2)	-	-	-
ν(C=O) ester		1642 (s)	
ν(C=O···H) ester			
ν(C=O···H weak) acid	1727 (vs)		
ν(C=O···H strong) acid			
ν(C=C) phenolic acid	1615 (vs)		
ν(C−C) aromatic			
ν(C−C) aromatic			
ν(C−C) aromatic (conjugated with C=C)	1500 (vw,sh)		
δ(CH_2) scissoring		1420 (m,b)	1435 (vs,b)
ν(C−C) aromatic (conjugated with C=C)	1424 (vw,sh)		
δ(CH_2) wagging and twisting	1350 (m,b)	1383 (w)	1380 (vw)
δ(OH)	1227 (s,b)	1153 (s)	1228 (vw)
ν_a(C−O−C), ester			
ν_s(C−O−C), ester			
ν(C−O−C), glycosydic bond	1051 (vs,b)	–	–
ν(CvO)	902 (vw)	857 (m)	
γ(C−H) aromatic	875 (w)		
δ(CH_2) rocking	632(s,b)	762 (m)	655 (m,b)

ν: stretching; δ: bending; γ: out of plane; a: asymmetric; s: symmetric s: strong; m: medium; w: weak; vs: very strong; vw: very weak; b: broad; sh: shoulder

4. Conclusion

A modified nanoprecipitation method was successfully implemented for the preparation of the MD-APPE NPs and RSM was utilized for the process conditions modeling and optimization. The results indicated that

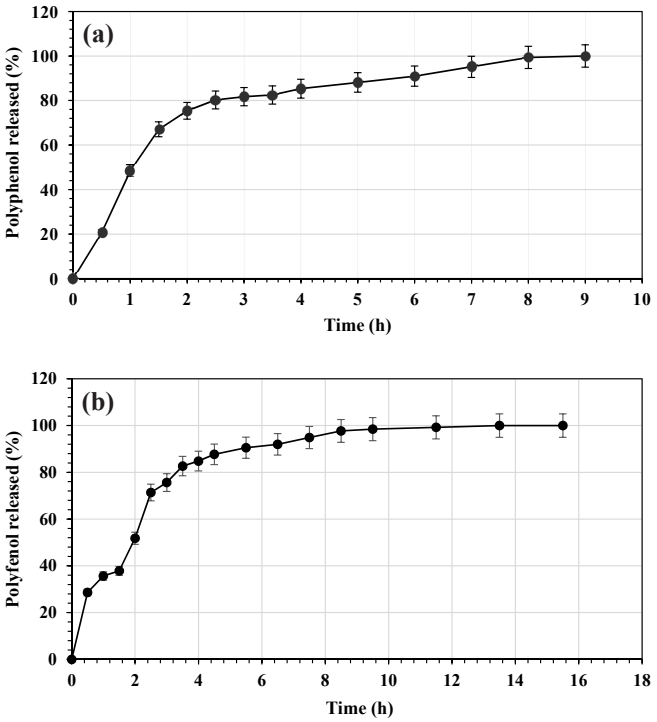

Fig. 5. In vitro release profile of MD-APPE NPs at pH 4.5 (a) and 6.8 (b).

the all the independent variables; i.e. the shell to core, the time of sonication homogenization, and the weight percentage of surfactant, were statistically significant factors affecting both the acquired TPC loading efficiency within the MD and nanoparticle formation yield. In the optimal condition, NPs with a mean average size of 52 nm with the distribution width of 40 nm and high loading efficiency of 98% were produced. The scientific basis of our hypothesis was strengthened by the use of FT-IR spectrums, DLS measurement and FE-SEM image and in vitro release studies.

Future studies include the stability and shelf life of the final product during food processing operating conditions, such as pH fluctuations in different finished products and thermal treatment during pasteurization and sterilization.

Acknowledgment

The authors wish to thank the Iran Nanotechnology Initiative Council (INIC) for partial financial support and the staff of the Department of Chemical Technologies at the Iranian Research Organization for Science and Technology (IROST), and mostly Dr. Bashiri Sadr for their co-operation and support. We also appreciate the efforts of Sanich Co. for providing the apple industrial wastes.

References

[1] J. Boyer, R.H. Liu, Apple phytochemicals and their health benefits, Nutr. J. 3 (2004) 1-15.

[2] B. Suárez, Á.L. Álvarez, Y.D. Garc'ia, G. del Barrio, A.P. Lobo, F. Parra, Phenolic profiles, antioxidant activity and in vitro antiviral properties of apple pomace, Food Chem. 120 (2010) 339-342.

[3] G.S. Dhillon, S. Kaur, S.K. Brar, Perspective of apple processing wastes as low-cost substrates for bioproduction of high value products: A review, Renew. Sust. Energ. Rev. 27 (2013) 789-805.

[4] Z. Fang, B. Bhandari, Encapsulation of polyphenols-a review, Trends Food Sci. Tech. 21 (2010) 510-523.

[5] O.I. Parisi, F. Puoci, D. Restuccia, G. Farina, F. Iemma, N. Picci, Polyphenols and their formulations: Different strategies to overcome the drawbacks associated with their poor stability and bioavailability, in: Polyphenols in Human Health and Disease, Elsevier Academic Press, USA, 2014, pp. 29-45.

[6] G. Spigno, F. Donsì, D. Amendola, M. Sessa, G. Ferrari, D.M. De Faveri, Nanoencapsulation systems to improve solubility and antioxidant efficiency of a grape marc extract into hazelnut paste, J. Food Eng. 114 (2013) 207-214.

[7] H.B. Nair, B. Sung, V.R. Yadav, R. Kannappan, M.M. Chaturvedi, B.B. Aggarwal, Delivery of antiinflammatory nutraceuticals by nanoparticles for the prevention and treatment of cancer, Biochem. Pharmacol. 80 (2010) 1833-1843.

[8] H. Souguir, F. Salaün, P. Douillet, I. Vroman, S. Chatterjee, Nanoencapsulation of curcumin in polyurethane and polyurea shells by an emulsion diffusion method, Chem. Eng. J. 221 (2013) 133-145.

[9] A. Altunbas, S.J. Lee, S.A. Rajasekaran, J.P. Schneider, D.J. Pochan, Encapsulation of curcumin in self-assembling peptide hydrogels as injectable drug delivery vehicles, Biomaterials, 32 (2011) 5906-5914.

[10] P. Salehi, O.V. Akinpelu, S. Waissbluth, E. Peleva, B. Meehan, J. Rak, S.J. Daniel, Attenuation of cisplatin ototoxicity by otoprotective effects of nanoencapsulated curcumin and dexamethasone in a guinea pig model, Otol. Neurotol. 35 (2014) 1131-1139.

[11] S. Ghosh, S.R. Dungdung, S.T. Chowdhury, A.K. Mandal, S. Sarkar, D. Ghosh, N. Das, Encapsulation of the flavonoid quercetin with an arsenic chelator into nanocapsules enables the simultaneous delivery of hydrophobic and hydrophilic drugs with a synergistic effect against chronic arsenic accumulation and oxidative stress, Free Radical Bio. Med. 51 (2011) 1893-1902.

[12] L. Dian, E. Yu, X. Chen, X. Wen, Z. Zhang, L. Qin, Q. Wang, G. Li, C. Wu, Enhancing oral bioavailability of quercetin using novel soluplus polymeric micelles, Nanoscale Res. Lett. 9 (2014) 684, 11 pages.

[13] A.R. Patel, P.C.M. Heussen, J. Hazekamp, E. Drost, K.P. Velikov, Quercetin loaded biopolymeric colloidal particles prepared by simultaneous precipitation of quercetin with hydrophobic protein in aqueous medium, Food Chem. 133 (2012) 423-429.

[14] C.F. Rodrigues, K. Ascencao, F. A.M. Silva, B. Sarmento, M. B.P.P. Oliveira, J.C. Andrade, Drug-delivery systems of green tea catechins for improved stability and bioavailability, Curr. Med. Chem. 20 (2013) 4744-4757.

[15] S.M. Henning, Y. Niu, Y. Liu, N.H. Lee, Y. Hara, G.D. Thames, R.R. Minutti, C.L. Carpenter, H. Wang, D. Heber, Bioavailability and antioxidant effect of epigallocatechin gallate administered in purified form versus as green tea extract in healthy individuals, J. Nutr. Biochem. 16 (2005) 610-616.

[16] Anonymous, Agricultural statistics Volume III - horticultural crops, Tehran, 2014.

[17] C.M. Galanakis, Recovery of high added-value components from food wastes: Conventional, emerging technologies and commercialized applications, Trends Food Sci. Tech. 26 (2012) 68-87.

[18] S. Faramarzi, A. Yadollahi, M. Barzegar, K. Sadraei, S. Pacifico, T. Jemric, Comparison of Phenolic compounds' content and antioxidant activity between Some Native Iranian apples and standard cultivar "Gala", J. Agr. Sci. Tech.-Iran, 16 (2014) 1601-1611.

[19] J. Ubbink, J. Krüger, Physical approaches for the delivery of active ingredients in foods, Trends Food Sci. Tech. 17 (2006) 244-254.

[20] C.E. Mora-huertas, H. Fessi, A. Elaissari, Polymer-based nanocapsules for drug delivery, Int. J. Pharm. 385 (2010) 113-142.

[21] R. Harris, E. Lecumberri, I. Mateos-Aparicio, M. Mengíbar, A. Heras, Chitosan nanoparticles and microspheres for the encapsulation of natural antioxidants extracted from *Ilex paraguariensis*, Carbohyd. Polym. 84 (2011) 803-806.

[22] F. Avaltroni, P.P.E. Bouquerand, V. Normand, Maltodextrin molecular weight distribution influence on the glass transition temperature and viscosity in aqueous solutions, Carbohyd. Polym. 58 (2004) 323-334.

[23] E.K. Bae, S.J. Lee, Microencapsulation of avocado oil by spray drying using whey protein and maltodextrin, J. Microencapsul. 25 (2008) 549-560.

[24] H. Fessi, F. Puisieux, J.P. Devissaguet, N. Ammoury, S. Benita, Nanocapsule formation by interfacial polymer deposition following solvent displacement, Int. J. Pharm. 55 (1989) 1-4.

[25] S. Khoee, M. Yaghoobian, An investigation into the role of surfactants in controlling particle size of polymeric nanocapsules containing penicillin-G in double emulsion, Eur. J. Med. Chem. 44 (2009) 2392-2399.

[26] S. Saikia, N.K. Mahnot, C.L. Mahanta, Optimisation of phenolic extraction from *Averrhoa carambola* pomace by response surface methodology and its microencapsulation by spray and freeze drying, Food Chem. 171 (2015) 144-152.

[27] G.B. Celli, A. Ghanem, M.S.-L. Brooks, Optimized encapsulation of anthocyanin-rich extract from haskap berries (*Lonicera caerulea* L.) in calcium-alginate microparticles, J. Berry Res. 6 (2016) 1-11.

[28] M. Pinelo, M. Rubilar, M. Jerez, J. Sineiro, M.J. Núñez, Effect of solvent, temperature, and solvent-to-solid ratio on the total phenolic content and antiradical activity of extracts from different components of grape pomace, J. Agr. Food Chem. 53 (2005) 2111-2117.

[29] Q. Wang, S. Ma, B. Fu, F.S.C. Lee, X. Wang, Development of multi-stage countercurrent extraction technology for the extraction of glycyrrhizic acid (GA) from licorice (*Glycyrrhiza uralensis* Fisch), Biochem. Eng. J. 21 (2004) 285-292.

[30] M. Valipour, Process conditions optimization in the polyphenolic extraction (one- and multi-counter current) from Iranian industrial apple pomace, Chemistry MSc thesis, Iranian Research Organization for Science and Technology (IROST), 2016.

[31] U. Bilati, E. Allémann, E. Doelker, Development of a nanoprecipitation method intended for the entrapment of hydrophilic drugs into nanoparticles, Eur. J. Pharm. Sci. 24 (2005) 67-75.

[32] S. Galindo-Rodriguez, E. Allémann, H. Fessi, E. Doelker, Physicochemical parameters associated with nanoparticle formation in the salting-out, emulsification-diffusion, and nanoprecipitation methods, Pharm. Res. 21 (2004) 1428-1439.

[33] S.A. Guhagarkar, V.C. Malshe, P. V Devarajan, Nanoparticles of polyethylene sebacate: A new biodegradable polymer, AAPS PharmSciTech. 10 (2009) 935-942.

[34] M.E. Matteucci, M.A. Hotze, K.P. Johnston, R.O. Williams, Drug nanoparticles by antisolvent precipitation: Mixing energy versus surfactant stabilization, Langmuir, 22 (2006) 8951-8959.

[35] M.R. Kulterer, M. Reischl, V.E. Reichel, S. Hribernik, M. Wu, S. Köstler, R. Kargl, V. Ribitsch, Nanoprecipitation of cellulose acetate using solvent/nonsolvent mixtures as dispersive media, Colloid. Surface. A 375 (2011) 23-29.

[36] E. Lepeltier, C. Bourgaux, P. Couvreur, Nano-precipitation and the "Ouzo effect": Application to drug delivery devices, Adv. Drug Deliver. Rev. 71 (2014) 86-97.

[37] K. Fernández, J. Aburto, C. von Plessing, M. Rockel, E. Aspé, Factorial design optimization and characterization of poly-lactic acid (PLA) nanoparticle formation for the delivery of grape extracts, Food Chem. 207 (2016) 75-85.

[38] A.B. Shirode, D.J. Bharali, S. Nallanthighal, J.K. Coon, S.A. Mousa, and R. Reliene, Nanoencapsulation of pomegranate bioactive compounds for breast cancer chemoprevention, Int. J. Nanomed. 10 (2015) 475-484.

[39] J.A. Heredia-Guerrero, J.J. Benìtez, E. Domìnguez, I.S. Bayer, R. Cingolani, A. Athanassiou, A. Heredia, Infrared and Raman spectroscopic features of plant cuticles: A review, Front. Plant Sci. 5 (2014) 305.

[40] S.K. Pandey, D.K. Patel, R. Thakur, D.P. Mishra, P. Maiti, C. Haldar, Anti-cancer evaluation of quercetin embedded PLA nanoparticles synthesized by emulsified nanoprecipitation, Int. J. Biol. Macromol. 75 (2015) 521-529.

[41] E.S. Lee, Z. Gao, Y.H. Bae, Recent progress in tumor pH targeting nanotechnology, J. Control. Release, 132 (2008) 164-170.